
Axion Telescope Experiment

MINOWA, Makoto

*Department of Physics and Research Center for the Early Universe (RESCEU),
School of Science, The University of Tokyo, 7-3-1 Hongo, Bunkyo-ku, Tokyo 113-0033, Japan*

Abstract

We have constructed a long superconducting magnet called the axion telescope to search for axions which could have been produced in the solar core or other various celestial objects by exploiting their conversion to x-rays in the magnetic field. The axion telescope is equipped with PIN-photodiode x-ray detectors at the end and an altazimuth mount to track the object.

We put a limit on axion-photon coupling constant by the search for the solar axions. The limit is more stringent than the limit inferred from the solar age consideration and also more stringent than the recent helioseismological bound. We also put limits on the axion flux coming from the various celestial objects for the first time by the ground-based direct search.

1. Introduction

The axion is a light neutral pseudoscalar particle yet to be discovered. It was introduced to solve the strong CP problem[1, 2].

The expected property of the axion is characterized mostly by its mass, m_a . If $10^{-5} < m_a < 10^{-3}$ eV, the axion can be copiously produced in the early universe so that they can close the universe. Another astrophysically interesting mass region is at around one to a few eV. Such axions can be allowed for some harmonic axion models by other astrophysical or cosmological constraints. In this region, the axion would be produced in the solar core through the Primakoff effect. It has an energy spectrum very similar to that of black body radiation photons with an average energy of about 4 keV[3, 4]. It can be converted back to an x-ray in a strong magnetic field in the laboratory by the inverse process. The principle of the production and detection is illustrated in Fig. 1..

The conversion rate is given by:

$$P_{a \rightarrow \gamma} = \frac{g_{a\gamma\gamma}^2}{4} \left| \int_0^L B e^{iqz} dz \right|^2 \quad (1)$$

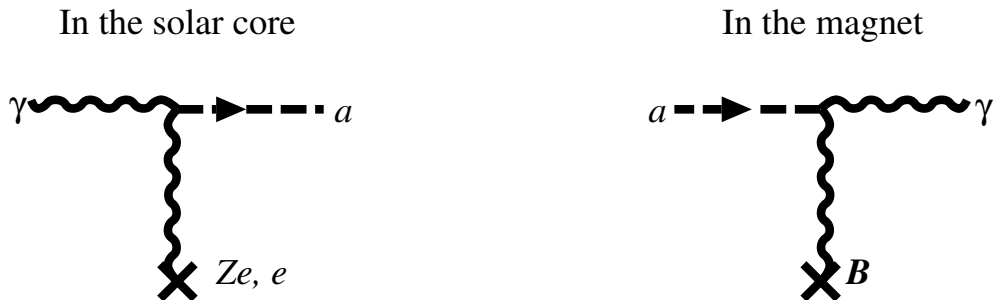


Fig. 1. The solar axions produced via the Primakoff process in the solar core are, then, reconverted into x rays via the reverse process.

where $g_{a\gamma\gamma}$ is the axion-photon coupling constant, z is the coordinate along the incident solar axion, B is the strength of the magnetic field, L is the length along the z -axis, and $q = |(m_\gamma^2 - m_a^2)/2E|$ is the momentum transfer by the virtual photon. Here, m_γ is the effective mass of the photon which is of course zero in vacuum. For heavier axions, momentum transfer, q , becomes not negligible, thus the sensitivity of the detector is lost. Coherence can, however, be restored by filling the conversion region with buffer gas since a photon of x-ray region has an effective mass in a medium. For light gas, such as hydrogen or helium, it is simply written as:

$$m_\gamma = \sqrt{\frac{4\pi\alpha N_e}{m_e}}. \quad (2)$$

We search for such x-rays coming from the direction of the sun with a newly developed instrument called the axion telescope.

2. Axion Helioscope

A schematic view of the helioscope is shown in Fig. 2.. It consists of three parts, a tracking system, superconducting coils and x-ray detectors. The tracking system is an altazimuth mount and drives a 3-m long vacuum cylinder of the helioscope to track the sun. Its trackable altitude ranges from -28° to $+28^\circ$ and almost any azimuthal direction is trackable. This view range corresponds to about 50% of duty cycle for the sun measurement in Tokyo. The other half of a day we measure the background. This helioscope mount is driven by two AC servo motors controlled by a personal computer (PC) through CAMAC bus. The PC regularly monitors two precision rotary encoders through CAMAC bus and forms a feedback control loop. The directional origin of the helioscope was measured using a theodolite. The azimuthal origin is determined from the observed direction

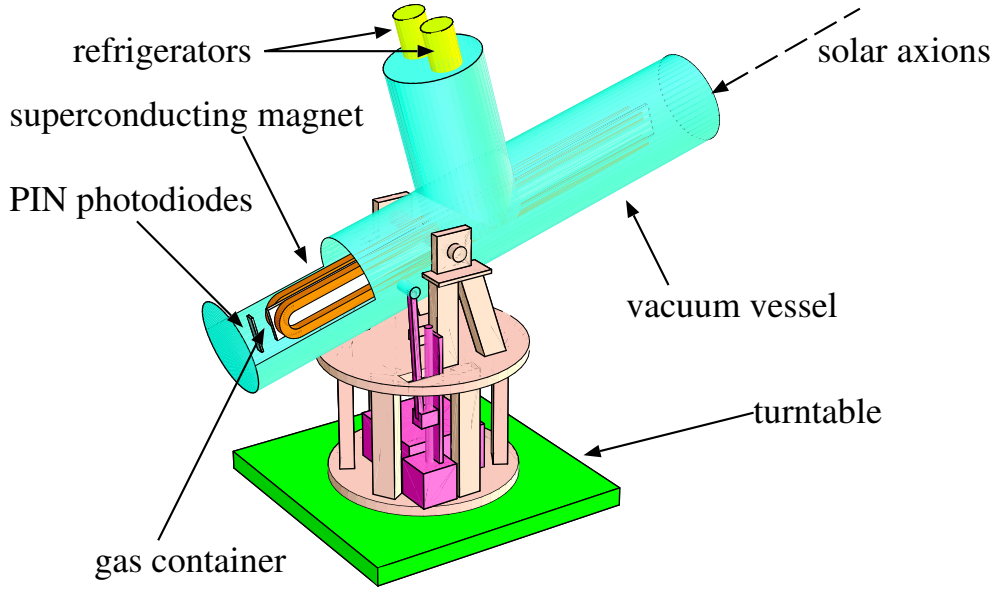


Fig. 2. The schematic view of the axion helioscope.

of Polaris and the absolute altitude is determined from a spirit level.

The superconducting coils and the x-ray detector are mounted in the cylinder. The aperture volume between the coils is $2300(L) \times 92(H) \times 20(W)$ mm³ and the magnetic field strength in the aperture is 4 T. The coils are kept at 5–6 K during operation. They are directly cooled with two Gifford-McMahon refrigerators and no cryogen is needed. The magnet has also a persistent current switch. After excitation, it is switched into persistent current mode and the current leads are taken away. The details of this cryogen-free superconducting magnet are described elsewhere[5].

Sixteen PIN photodiodes, Hamamatsu Photonics S3590-06, are used as the x-ray detectors(Fig. 3.). The chip size is $11 \times 11 \times 0.5$ mm³. Each chip is mounted on a Kapton film bonded to an Invar plate with cryogenic compatible adhesive. The x-ray detectors are mounted in a radiation shielding box made of oxygen-free high conductivity copper (OFHC Cu) which is operated at about 60 K. The copper shield is surrounded by a lead shield which is at room temperature.

The output from each photodiode is fed to a charge sensitive preamplifier whose first-stage FET is at the cryogenic stage near the photodiode chip and the preamplifier outputs are digitized using flash analog-to-digital converters (FADC's), REPIC RPC-081's. We performed numerical pulse shaping to the raw waveform using the Wiener filter. The energy of an x ray is given by the peak height of a wave after shaping. Each detector was calibrated by 6-keV manganese

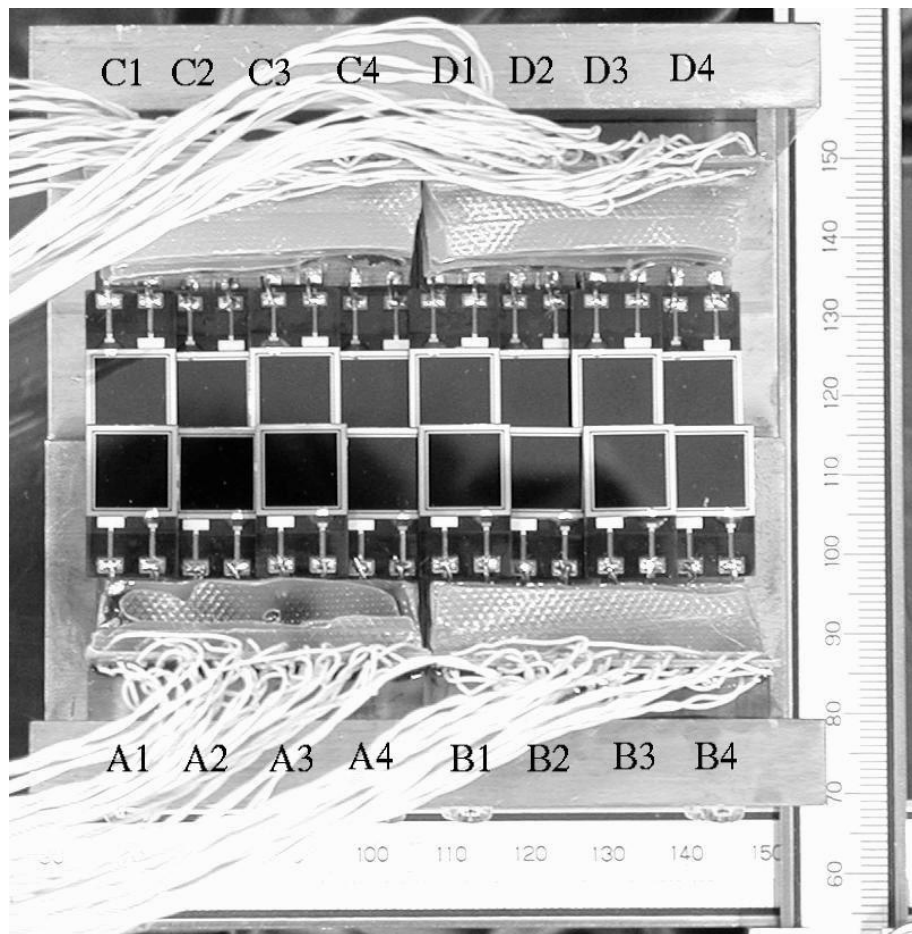


Fig. 3. 16 PIN photodiodes and head parts of th preamplifiers.

x ray from a ^{55}Fe source which can be exposed to the detector and hidden behind the shield during the measurement. The energy resolutions for 6-keV photon was 0.8–1 keV (FWHM).

3. Solar Axion Search

In the first stage of the solar axion search experiment, no buffer gas was used in the magnetic field region. The measurement consists of two parts, the solar observation and the background measurement. While the sun is in the trackable range, the helioscope is directed to the sun. For the rest of the time, the background spectrum was measured. The U.S. Naval Observatory Vector Astronomy Subroutines (NOVAS) [7] was used to calculate the sun position.

From the absence of the axion signal, an upper limit to the axion-photon coupling was set to be $g_{a\gamma\gamma} < 6.0 \times 10^{-10} \text{GeV}^{-1}$ (95% CL) for $m_a < 0.03 \text{eV}$. The result is published in [6]. The upper limit is shown in Fig. 4. as a function of m_a . The limits from the second stage experiment are plotted together. There are also some other bounds plotted in the same figure. The SOLAX [8] is a solar axion experiment which exploits the coherent conversion on the crystalline planes in a germanium detector. The limit $g_{a\gamma\gamma} < 2.3 \times 10^{-9} \text{GeV}^{-1}$ is the solar limit inferred from the solar age consideration. The limit $g_{a\gamma\gamma} < 1 \times 10^{-9} \text{GeV}^{-1}$ is a new solar limit recently reported[9]. Above this line, standard solar models with energy losses by solar axions cannot fit to the helioseismological sound-speed profile. Our upper limit is the first to go lower than these two solar limits in this mass region.

In the second stage of the search experiment, the convergence region was filled with the buffer gas to retain the coherence of the convergence of the heavier mass axions.

The new device introduced this time is the gas container. We adopted cold helium gas as the dispersion-matching medium. Light gas is preferred since it minimizes x-ray absorption by the gas. Helium has another virtue that it remains at gas state at 5 K, the same temperature as the coil. At 5 K, the gas pressure corresponding to our ultimate goal, $m_a = 2.6 \text{eV}$, reaches only 0.13 MPa. The container body is made of four stainless steel square pipes welded to each other. The entire container body is wrapped with 5N high purity aluminium sheet to achieve high uniformity of temperature. At the end of the container, gas is separated from vacuum with an x-ray window which is transparent to x ray above 2 keV and can hold gas up to 0.3 MPa at liquid helium temperature.

The measurement with buffer gas was performed for ten photon mass settings to scan up to 0.26 eV.

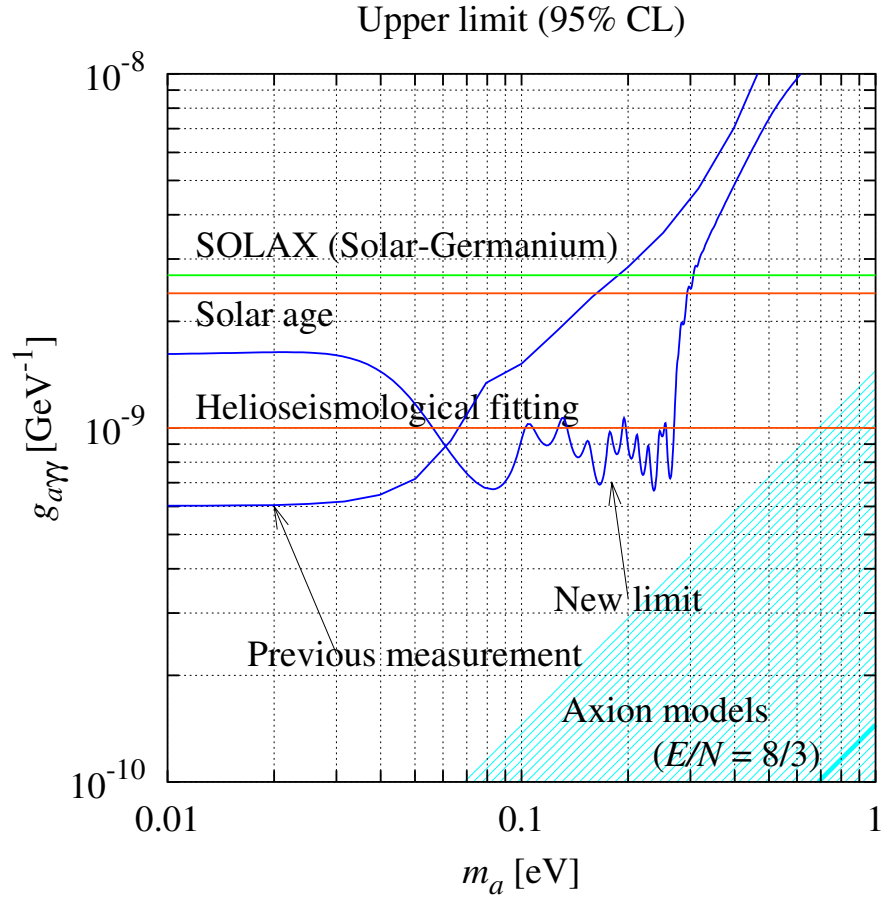


Fig. 4. The exclusion plot on $g_{a\gamma\gamma}$ to m_a at 95% confidence level is plotted where some other bounds are plotted together. The limit from the first stage experiment without buffer gas is shown as “Previous measurement”. “New limit ” corresponds to the second stage experiment with buffer gas. Dashed lines are the limit by SOLAX experiment, the limit inferred from the solar age consideration, and the recent helioseismological bound. The hatched area is the preferred axion models. The thick line corresponds to the case when a simple GUT is assumed.

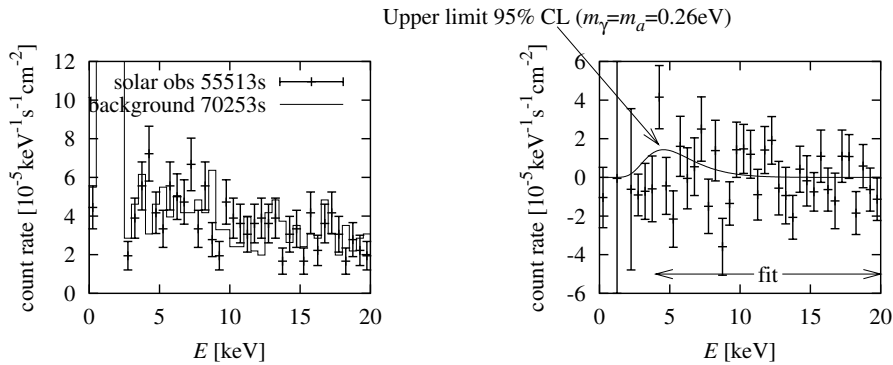


Fig. 5. The left figure shows the energy spectrum of the solar observation (error bars) and the background spectrum (solid line) when the gas density was tuned to $m_\gamma = 0.26\text{eV}$. The right figure shows the net energy spectrum of the left where the background is subtracted from the solar observation.

In Fig. 5., one of the energy spectra of the solar observation is shown together with the background spectrum. We searched for expected axion signals which scales with $g_{a\gamma\gamma}^4$ for various m_a in these spectra. The smooth curve in the figure represents an example for the expected axion signal for $m_a = m_\gamma = 0.26\text{eV}$ and $g_{a\gamma\gamma} = 7 \times 10^{-10}\text{GeV}^{-1}$.

In the analysis, the ten measurements with the ten different gas densities are combined together by using the total χ^2 . The energy region 4–20 keV was used for fitting. Since no significant excess was seen for any m_a , we set upper limit on $g_{a\gamma\gamma}$ at 95% confidence level using the Bayesian method. In Fig. 4., upper limits on $g_{a\gamma\gamma}$ are plotted as a function of m_a . The result is published in [10].

Again, our limits are better than the limit inferred from the solar age consideration. They are also better than the helioseismological limit except in a small fraction of the mass region.

4. Other Axion Emitting Stellar Objects

Our helioscope is not necessarily only for the sun. In principle, it can be used to search for the axions from other stellar objects.

The arguments on the solar axion can be applied to other stars and axion luminosity of them can be calculated[11]. Compact objects like white dwarfs, neutron stars and black holes can also be the axion sources in two aspects. One is the thermal emissions from the objects themselves and another is the thermal emissions from their accretion disks. Axion luminosity of the thermal emission from the objects is calculated[12, 13] although axion luminosity from the accretions are

not calculated.

Similar to neutrinos, the supernova explosion liberates its energy in the form of the axions [14, 15, 16]. The gamma ray bursts, which are the most violent explosions in the universe, are also the candidate. However, it is rather hard to observe these two objects by our apparatus because we do not know where to see in advance of the occurrence.

Except for the solar axion search, no ground-based celestial search experiments have been reported by now. There exist some observational constraints on $g_{a\gamma\gamma}$ extracted from the analyses of satellite x-ray observations[17, 14, 15, 16]. These limits are very stringent but valid only for a massless or a very light pseudoscalar, since the long conversion field requires strict coherency.

We show here the preliminary results of the celestial axion search experiments done by directing the axion helioscope toward the possible sources. During the search, no buffer gas was used in the magnetic field region. Our search consists of two methods. The one is the celestial scan. Fig.6. shows the region of the scan in the galactic coordinate.

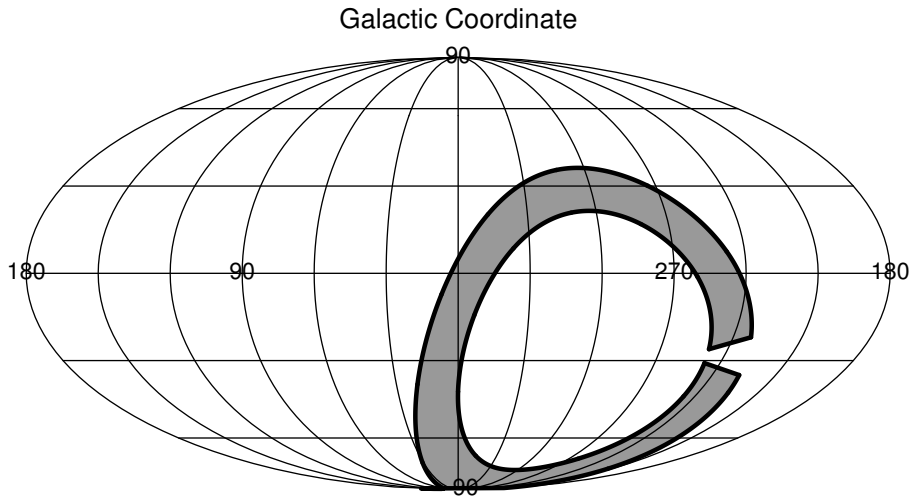


Fig. 6. The constrained region in the galactic coordinate. The shaded area is the constrained region. This region occupies about 10 % of the celestial sphere.

We scanned 10 % of the celestial sphere by the apparatus, and found no apparent signals. By assuming that the axion energy distribution is flat in 4–20 keV, the 95 % confidence limit on the differential flux is $d\Phi_a/dE_a < 3.3 \times 10^{16} \text{ keV}^{-1}\text{s}^{-1}\text{cm}^{-2}$ for 4–20 keV, provided the axion mass of $m_a < 0.03 \text{ eV}$ and the axion-to-photon coupling of $g_{a\gamma\gamma} = 10^{-10} \text{ GeV}^{-1}$.

The other is the tracking. We examined the galactic center, Scorpius X-1,

Vela X-1 and Crab nebula by tracking these objects. The results are 10^2 – 10^3 more stringent than the scan result.

These results are the first reliable constraints for the axion emission from celestial objects other than the sun. Since the distances to the sources are very long, these limits are higher than the theoretically predicted values. However, these results give reliable informations for the celestial objects whose theories have much uncertainty, and can be strong constraints for exotic objects which might be proposed in the future.

5. Conclusion

We have developed the axion helioscope. The solar axion with mass up to 0.26eV has been searched for. But no evidence for the axion was seen. New upper limit on $g_{a\gamma\gamma}$ which ranges 6.0 – $9.6 \times 10^{-10} \text{GeV}^{-1}$ was set for $m_a < 0.26 \text{eV}$, which is far more stringent than the solar existence limit and is also more stringent than the recent helioseismological bound. This experiment is currently the only one existing experiment which has enough sensitivity to detect such solar axion that do not violate the solar model itself.

We also put limits on the axion flux coming from the various celestial objects for the first time by the ground-based direct search.

Acknowledgments

This research is supported by the Grant-in-Aid for COE research by the Japanese Ministry of Education, Science, Sports and Culture, by the Grant-in-Aid for scientific research by the Japan Society for the Promotion of Science, and also by the Matsuo Foundation. This work is done in collaboration with Y. Inoue, T. Namba, S. Moriyama, Y. Takasu, T. Horiuchi, and A. Yamamoto.

References

- [1] R.D. Peccei, H.R. Quinn, Phys. Rev. Lett. 38 (1977) 1440; Phys. Rev. D 16 (1977) 1791; S. Weinberg, Phys. Rev. Lett. 40 (1978) 223; F. Wilczek, Phys. Rev. Lett. 40 (1978) 279.
- [2] J.E. Kim, Phys. Rep. 150 (1978) 1; M.S. Turner, Phys. Rep. 198 (1990) 67; L.J Rosenberg, K. van Bibber, Phys. Rep. 325 (2000) 1; G.G. Raffelt, Phys. Rep. 333-334 (2000) 593.
- [3] P. Sikivie, Phys. Rev. Lett. 51 (1983) 1415.
- [4] K. van Bibber *et al.*, Phys. Rev. D 39 (1989) 2089.

- [5] Y. Sato, K. Makishima, S. Mizumaki, A. Yamamoto, S. Moriyama, Y. Inoue, M. Minowa, T. Namba, Y. Takasu, Development of A Cryogen-free Superconducting Dipole Magnet, *the 15th International Conference on Magnet Technology* (MT-15, Beijing, October 20–24, 1997), and KEK-PREPRINT-97-202.
- [6] S. Moriyama, M. Minowa, Y. Inoue, T. Namba, Y. Takasu, and A. Yamamoto, *Phys. Lett. B* 434 (1998) 147.
- [7] G. H. Kaplan *et al.*, *Astronomical Journal* 97 (1989) 1197;
URL: <http://aa.usno.navy.mil/AA/software/novas/>.
- [8] A.O. Gattone, *et al.*, *Nucl. Phys. B(Proc. Suppl.)* 70 (1999) 59.
- [9] H. Schlattl, A. Weiss, and G. Raffelt, *Astropart. Phys.* 10 (1999) 353.
- [10] Y. Inoue, T. Namba, S. Moriyama, M. Minowa, Y. Takasu, T. Horiuchi, and A. Yamamoto, *astro-ph/0012338*.
- [11] E. D. Carlson, *Phys. Lett. B* 344 (1995) 245.
- [12] N. Iwamoto, *Phys. Rev. D* 53 (1984) 1198.
- [13] D. E. Morris, *Phys. Rev. D* 34 (1986) 843.
- [14] J. W. Brockway, E. D. Carlson, and G. G. Raffelt, *Phys. Lett. B* 383 (1996) 439.
- [15] E. Massó, *hep-ph/9704056*.
- [16] J. A. Grifols, E. Massó, and R. Toldrà, *Phys. Rev. Lett.* 77 (1996) 2372.
- [17] E. D. Carlson, and W. D. Garretson, 336 (1994) 431.